



Gene delivery and immunomodulatory effects of plasmid DNA associated with Branched Amphiphilic Peptide Capsules

L.A. Avila^{a,c,1}, L.R.M.M. Aps^{b,1}, N. Ploscariu^c, P. Sukthankar^{d,c}, R. Guo^e, K.E. Wilkinson^c, P. Games^f, R. Szoszkiewicz^g, R.P.S. Alves^b, M.O. Diniz^b, Y. Fang^e, L.C.S. Ferreira^b, J.M. Tomich^{c,*}

^a Department of Chemistry and Biochemistry, Auburn University, Auburn, AL 36849, USA

^b Institute of Biomedical Sciences, University of São Paulo, São Paulo, SP 05508-900, Brazil

^c Department of Biochemistry and Molecular Biophysics, Kansas State University, Manhattan, KS 66506-3902, USA

^d Department of Molecular Biosciences, Kansas University, Lawrence, KS 66045, USA

^e Department of Diagnostic Medicine & Pathobiology, College of Veterinary Medicine, Kansas State University, Manhattan, KS 66502, USA

^f Department of General Biology, Federal University of Viçosa, Viçosa, MG 36570-900, Brazil

^g Faculty of Materials Science and Engineering, Warsaw University of Technology, Warsaw 02-507, Poland

ARTICLE INFO

Article history:

Received 25 July 2016

Received in revised form 27 August 2016

Accepted 31 August 2016

Available online 1 September 2016

Keywords:

Cationic branched peptides

BAPCs

Peptide-DNA interactions

DNA vaccine

In vivo gene delivery

HPV

Anti-cancer vaccine

Biocompatible material

ABSTRACT

We recently reported on a new class of branched amphiphilic peptides that associate with double stranded DNA and promote in vitro transfection of eukaryotic cells. In the present study, we tested a different formulation in which plasmid DNA associates with the surface of preformed 20–30 nm cationic capsules formed through the self-assembly of the two branched amphiphilic peptides. Under these conditions, the negatively charged DNA interacts with the cationic surface of the Branched Amphiphilic Peptide Capsules (BAPCs) through numerous electrostatic interactions generating peptide-DNA complexes with sizes ranging from 50 to 250 nm. The BAPCs-DNA nanoparticles are capable of delivering plasmid DNA of different size into cells in culture, yielding high transfection rates and minimal cytotoxicity. Furthermore, BAPCs were tested for in vivo delivery of a DNA vaccine previously designed to activate immune responses and capable of controlling tumors induced by type 16 human papilloma virus (HPV-16). The BAPCs-DNA nanoparticles enhanced the vaccine-induced antitumor protection and promoted activation of murine dendritic cells without significant toxic effects. These results indicate that branched amphiphilic oligo-peptides nanoparticles represent a new and promising nonviral DNA/gene delivery approach endowing immunomodulatory properties for DNA vaccines.

© 2016 Elsevier B.V. All rights reserved.

1. Introduction

Administration of exogenous DNA may promote in vivo gene transfection and protein expression that can be employed either for prophylactic or therapeutic purposes [1]. Association of DNA with molecular carriers can increase the number of transfected cells and, consequently, the amount of in vivo expressed protein [2,3]. Vaccinia virus and other poxviruses, retrovirus, adenovirus and herpes simplex virus are the most frequently used molecular carriers, particularly in gene therapy studies [4,5]. Nonetheless, viruses present several drawbacks regarding large scale clinical applications including induction of dangerous inflammatory reactions, generation of immune responses to the viral vector and size limitation on the DNA that can be packaged [6,7]. Biodegradable materials, including cationic lipids, polymeric vesicles [8,9], lipid vesicles [10] and peptide vesicles [11,12] represent safer and rather simple alternatives to virus-based gene delivery tools.

Self-assembling cationic branched peptide vesicles are emerging as an alternative gene delivery approach over lipid-based methods, featuring resistance to oxidation and thermal stability [13]. The peptides are relatively easy to synthesize, and can be modified with specific cell targeting ligands [14]. The Tomich group developed Branched Amphiphilic Peptide Capsules (BAPCs) composed of two branched peptides: bis(Ac-FLIVIGSII)-K-K₄ and bis(Ac-FLIVI)-K-K₄ derived from a human transmembrane channel sequence [15,16]. These self-assembling peptides form hollow capsules in water displaying a uniform size of ~20–30 nm that can trap solutes during the capsule formation process [17]. In addition to small solutes, BAPCs can also encapsulate proteins, such as cytochrome c and RNase A [18]. “Conformationally constrained” 20–30 nm BAPCs are prepared using temperature shifts during the annealing process and, in a previous publications [19], we named them “locked” nano-capsules.

Early attempts to encase DNA during the assembly of the monomeric branched peptides following the procedure designed for the encapsulation of small solutes failed. Larger molecules such as plasmid DNA prevented capsule formation, generating different structures depending on the peptide/DNA molar ratios [20]. At high peptide/DNA ratios,

* Corresponding author.

E-mail address: jtomich@ksu.edu (J.M. Tomich).

¹ These authors contributed equally to this work.

excess peptide coated the plasmid surface, forming nano-fibers (0.5–1 μm in length), while at low ratios, the peptides promoted DNA condensation into nano-sized spherical structures (100–400 nm). The elongated structures were not effective in transfecting HeLa cells, however gene delivery efficiency of 20% was observed with the condensed structures [20].

In contrast, for this study we complexed DNA with preformed BAPCs following a different methodology. Pre-formed water filled “conformationally constrained” BAPCs acted as nucleation centers for the DNA molecules that coat the surface of the peptide capsules. Transfection of HeLa cells with “conformationally constrained” BAPC/GFP-encoding plasmid complexes generated higher transfection rates than commercially available transfection reagents, such as Lipofectin®, while showing significantly lower cytotoxic effects.

Although some transfection reagents display high gene delivery efficiencies *in vitro*, they often fail to produce equivalent results for *in vivo* applications [21]. In order to test the effectiveness of our system *in vivo*, we coated the “conformationally constrained” BAPCs with a DNA vaccine encoding an oncoprotein of the type 16 human papillomavirus (HPV-16) [22]. Mice vaccinated with DNA-coated BAPCs delayed tumor growth without detectable acute toxicity but at a peptide:DNA ratio different than that observed for optimal *in vitro* cell transfection. The complexes were able to activate mouse dendritic cells and showed clear immunomodulatory effects. In summary, the results presented here indicate that nano-sized BAPCs-DNA particles provide a less cytotoxic and efficient non-viral DNA/gene delivery approach for *in vitro* and *in vivo* applications.

2. Materials and methods

2.1. Peptide synthesis

The peptides bis(FLIVIGSII)-K-K₄ and bis(FLIVI)-K-K₄, were synthesized and cleaved as previously described [15] and then lyophilized before storing at room temperature (RT). The cleaved peptides were purified by reversed phase HPLC and characterized using matrix-assisted laser desorption ionization-time of flight (MALDI-TOF) mass spectrometry (Ultraflex II, MALDI TOF/TOF, Bruker Daltronics, Billerica MA) (Fig. 1S).

2.2. “Conformationally constrained” BAPC nanoparticle preparation

The peptides, were dissolved individually in pure 2,2,2-Trifluoroethanol (TFE) and their concentrations determined based on the absorbance of the phenylalanines at 258 nm [15]. Final concentrations of 500 μM were then prepared before removing the solvent under vacuum. Under these conditions the peptides remain as monomers during the drying process. Water was added drop-wise to the dried peptide mixture and allowed to stand for 30 min at 25 °C to form the water-filled nanocapsules. Subsequently, the solution was cooled to 4 °C, and incubated for 1 h prior to returning them to room temperature for an additional 30 min. This protocol yields the conformationally constrained BAPCs (20–30 nm), which are resistant to disassembly in the presence of organic solvents [19]. The peptide capsules were prepared in water (salt/buffer-free) to optimize the electrostatic interactions between the poly-anionic DNA and the cationic surface of the capsules. BAPCs prepared using other assembly temperature regimes do not work well in delivering nucleotides.

2.3. Preparation of DNA-BAPCs nanoparticles

For all peptide-DNA complex preparations different (N:P) charge ratios were tested. For instance, 1 mL of a 20 μM peptide concentration contains 1.20×10^{16} peptide molecules. There are 4 lysines positively charged, therefore $1.20 \times 10^{16} (4) = 4.80 \times 10^{16} \text{NH}_3^+$ (N). In the case of DNA, 2.5 μg of 4.7 kb ds plasmid in 1 mL contains 4.94×10^{11} ds

plasmid molecules (Average M.W. of a DNA basepair = 650 Da), considering the phosphate molecules, $4.94 \times 10^{11} (2 \times 4700) = 4.67 \times 10^{15} \text{PO}_4^-$ (P). Therefore, $4.80 \times 10^{16}/4.67 \times 10^{15}$ yields a N:P of 10.4. For the *in vitro* transfection experiments conformationally constrained BAPCs were added to a pEGFP-N3 or pCMV-SD95-21-GFP plasmid solutions at the suitable (N:P) for each cell line. The plasmid pEGFP-N3 (4.7 kb) was obtained from Dr. Dolores Takemoto (Clontech, Mountain View, CA) and pCMV-SD95-90 21-GFP (19.4 kb) [23]. Solutions were mixed carefully with a pipette and allowed to stand for 10 min at RT before adding CaCl_2 , 1.0 mM final concentration. After an additional 30 min incubation period, the solution was added to the cell culture. CaCl_2 , alone at this concentration was analyzed and did not to enhance DNA uptake or expression.

2.4. STEM sample preparation

For transmission electron microscopy (TEM) DNA-BAPCs Nanoparticles were prepared as previously described prior to placing the sample on the TEM grid. The samples were negatively stained using a multi isotope 2% Uranyl acetate (Uranium bis(acetato)-O-dioxodihydrate) (Sigma-Aldrich, St. Louis, MO) aqueous solution. Sample solutions (6 μL) were spotted on to grids and allowed to air dry before loading it into the FEI Tecnai F20XT Field Emission Transmission Electron Microscope (FEI North America, Hillsboro, Oregon).

2.5. Atomic force microscopy (AFM)

Peptide-DNA samples, were deposited onto freshly cleaved mica substrates (Fig. 1). After 15 min of incubation, the sample was dried under nitrogen. AFM topography images of immobilized BAPCs-DNA complexes were acquired in air using the contact mode on an Innova Atomic Force Microscope (AFM) from Bruker, USA (Fig. 1). The AFM scanner was calibrated using a TGZ1 silicon grating from NT-MDT, USA. MLCT-E cantilevers with their respective nominal spring constants of 0.05 N/m and 0.1 N/m were used, with set point contact forces of 1 nN or less. The AFM topography data were attained by subtracting background then using a second order line by line fitting methods incorporated within the Gwyddion software [24].

2.6. Determination of zeta potential

The different N:P BAPCs-DNA complex ratios were prepared as previously described. Particle size and zeta-potentials for all samples were determined using a Zetasizer Nano ZS (Malvern Instruments Ltd., Westborough, MA). Samples were analyzed in CaCl_2 1 mM and all measurements were performed in triplicates.

2.7. Cell culture

HeLa and HEK-293 cells were purchased from ATCC (CCL-2) and maintained as a previously described [20].

2.8. *In vitro* plasmid transfection

For transfection experiments, 1×10^5 cells were seeded on 22 mm culture dishes; 24 h later at 60% confluence, all medium was removed from the wells and 800 μL of Opti-MEM® 1 Reduced Serum Media was added. Next, for HeLa cells 200 μL BAPCs-DNA nanoparticles at N:P ratios of 1.3, 2.6, 5.2, 10.4, 20.8 and 26 were added to cells. These N:P ratios correspond to peptide concentrations of 2.5, 5, 10, 20, 40 and 50 μM respectively mixed with 2.5 μg of pEGFP-N3. For HEK-293 cells, BAPCs-DNA nanoparticles corresponding to N:P ratios of 6.5, 13, 26 and 52 (12.5, 25, 50 and 100 μM respectively), were mixed with 2.5 μg of pCMV-SD95-21-GFP and added to cells. They were then incubated under normoxic conditions for 2–6 h. After the incubation period, media and transfection reagent were removed and replaced with 1 mL

of fresh DMEM containing 10% FBS in each well. The cells were returned to the incubator for 48 h. For the positive control, cells were transfected with Lipofectin® (Invitrogen, Carlsbad, CA), with adjusted conditions for optimal results in each cell line (Fig. 2S). Lipoplexes for HeLa cells were formed in 200 μ L of OptiMEM® I serum medium mixing 2.5 μ g of pDNA with 8 μ L of the transfection reagent. For HEK-293, 2.5 μ g of DNA was mixed with 12 μ L of the cationic lipid. The lipoplexes were added to the cells and allowed to incubate for 6 h at 37 °C. After this incubation period, media and transfection reagent were removed and replaced with 1 mL of fresh DMEM containing 10% FBS in each well. The cells were returned to the incubator for 48 h. Transfection efficiency was monitored by confocal microscopy and quantified by fluorescence activated cell sorting (FACS), FACSCalibur (Becton Dickinson, Grayson, GA). Propidium iodide (PI) was used to identify and then exclude dead cells from the analysis. Non transfected cells containing only DNA and CaCl₂ (1 mM) were used as a control. Data were analyzed using the FlowJo software V.10.1 (TreeStar, OR, USA).

2.9. Confocal laser scanning microscopy

Images were obtained using a confocal LSM 700 laser-scanning microscope (Carl Zeiss, Gottingen, Germany).

2.10. Cell viability assay *in vitro*

Cell viability was monitored by flow cytometry using the cell death exclusion PI. For HeLa cells cell viability was also analyzed using exclusion of the fluorescent dye trypan blue. 1×10^5 HeLa cells were seeded on 22 mm culture dishes; 24 h later at 60% confluence, all medium was removed from the wells and 800 μ L of Opti-MEM® I Reduced Serum Media was added. Next, 200 μ L BAPCs-DNA nanoparticles with N:P ratios = 1.3, 2.6, 5.2, 10.4, 20.8 and 26, mixed with 2.5 g of were added to cells and allowed to incubated under normoxic conditions for 2–6 h. After this incubation period, media and nanoparticles were removed and replaced with 1 mL of fresh DMEM containing 10% FBS in each well. The cells were returned to the incubator for 48 h before performing the analysis. The Lipofectin® (Invitrogen, Carlsbad, CA) control was used according to the protocol previously mentioned.

2.11. Mice

Female C57BL/6 mice at 8–10 weeks of age were supplied by the Faculty of Veterinary Medicine and Animal Science and housed at the Microbiology Department of the University of Sao Paulo. All procedures involving animal handling and treatment followed the recommendations for the proper use and care of laboratory animals from the University of Sao Paulo Ethics Committee.

2.12. DNA vaccine and immunization regimens

The plasmid DNA vaccine (5.6 kb, pgDE7 plasmid) used in these experiments encode the type 16 human papilloma virus (HPV-16) E7 oncoprotein genetically fused to the HSV-1 gD protein (pgDE7) that was described previously [22]. Pre-assembled conformationally constrained BAPCs were added to an aqueous DNA solution containing 40 μ g of the plasmid DNA vaccine, using 400, 800 and 3200 μ M of BAPCs to achieve N:P ratios of 1.3, 2.6 and 10.4 respectively. Each animal (4–5 per group) was inoculated with a final volume of 100 μ L i.m. divided in 50 μ L aliquots and delivered into both tibialis anterior muscle of the hind limb. The immunization was carried out 3 days after subcutaneous transplantation of 7.5×10^4 TC-1 cells, which express the HPV-16 E7 oncoprotein. The TC-1 tumor cells were suspended in 100 μ L of serum-free medium and injected into the left rear flank of the animals. Tumor development was checked by visual inspection and measured using a digital caliper twice a week for a period of 70 days. The animals were scored as tumor-bearing when the tumors reached a size of

approximately 2 mm in diameter. Survival rates were based on the percentage of animals with tumor volumes reaching up to 500 mm³ according to the formula: $1/2(\text{length} \times \text{width}^2)$ or 10 mm of length.

2.13. Intracellular cytokine staining (ICS)

Intracellular IFN- γ staining was performed using blood samples collected 14 days after the vaccine administration, according to previously described procedures [22]. The blood samples were treated for lysis of red blood cells and cultured at a concentration of 10^6 cells/well for 6 h at 37 °C in 96-well round bottom microtiter plates with 10 μ g/mL of Brefeldin A (GolgiPlug; BD Biosciences, CA, USA) in the presence or not of 3 μ g/mL of the E7-specific RAHYNIVTF peptide (amino acids 49–57). After incubation, the cells were stained with BB515-conjugated anti-CD8a antibody and after fixation and permeabilization, with PE-labeled anti-IFN- γ . The buffers and antibodies were purchased from BD Biosciences (CA, USA). The cells were examined by flow cytometry using a FACS Fortessa (BD Biosciences) and the data were analyzed using FlowJo software (TreeStar, OR, USA).

2.14. Activation of mouse dendritic cells (DC) *in vitro*

Spleens and lymph nodes from naïve C57BL/6 mice were collected, carefully macerated and washed with ice-cold MACS buffers (PBS, 0.5% bovine serum albumin, 2 mM EDTA). Large particulate matter was removed by passing the cell suspension through a cell strainer 70 μ m nylon membrane. After suspended in MACS buffer cells were incubated with MicroBeads (Miltenyi Biotec) conjugated to hamster anti-mouse CD11c monoclonal antibodies according to the manufacturer's protocols. Positively selected DCs containing >90% CD11c+ cells were stimulated for 48 h with PBS, DNA (10 μ g of pgDE7) and LPS at 100 ng/mL as a final medium concentration. Also, CD11c+ cells were stimulated at the same conditions with the BAPCs-DNA nanoparticles at N:P charge ratio of 1.3 using 10 μ g of pgDE7 and BAPCs at 100 μ M and an additional group containing only uncoated BAPCs at 100 μ M as a final concentration (BAPCs). Then, the tested substances and stained with anti-CD11c+ cells were stained with, anti-I-A[b] (anti-MHCII), anti-CD40, anti-CD80 and anti-CD86 conjugated to different fluorochromes (BD Biosciences). The cells were examined by flow cytometry using FACS LSR Fortessa (BD Biosciences) and data were analyzed using the FlowJo software V.10.1 (TreeStar, OR, USA).

2.15. Cytometric bead array (CBA)

The cytokines levels in supernatants of dendritic cell cultures were measured after 48 h of stimulation using the CBA kit 200 Th1/Th2/Th17 (BD Biosciences) for the quantification of IL-2, IL-4, IL-6, INF-, TNF- α , IL-17A and IL-10 according to the manufacturer's instructions. In brief, the sample and the cytokine kit standards were mixed with microspheres coated with capture antibodies specific for the respective cytokines. Then, samples were incubated with the detection antibody labeled with phycoerythrin (PE) for 2 h at room temperature in the dark. The flow cytometry analysis was based on the fluorescence intensity using FACS Fortessa (BD Biosciences). Data were analyzed with the aid of the FCAP Array 3.0 to determine the concentration (pg/mL) and means of fluorescence intensities (MFI) of the samples and standards.

2.16. *In vivo* toxicity assay

Blood samples were collected individually from the submandibular plexus of mice 1 or 7 days after the immunization. Sera were obtained after centrifugation at 5000g at 4 °C for 30 min and measured for aspartate (AST) and alanine (ALT) transaminases (Laborclin, SP, and Brazil), lactate dehydrogenase (LDH), urea and creatinine (Wiener lab, Argentina) levels using commercial assay kits according to the manufacturer's protocols.

3. Results

3.1. Preparation and characterization of BAPCs-DNA nanoparticles

As previously reported [15], BAPCs preparation begins by mixing two peptides, bis(Ac-FLIVIGSII)-K-K₄ and bis(Ac-FLIVI)-K-K₄, at equimolar concentration in 2,2,2, Trifluoroethanol (TFE). In this solvent the peptides are monomeric, adopting a helical conformation, and do not aggregate. Once combined, the solvent is removed under vacuum and samples are then hydrated to form capsules of desired concentration by the dropwise addition of water. The capsules are kept for 30 min at 25 °C to reach a stable size of 20–30 nm, subsequently they are incubated at 4 °C for 1 h and then rewarmed to 25 °C thereby fixing their size (20–30 nm). The solution is allowed to stand at 25 °C for an additional 30 min before adding the dsDNA. Nanocapsules prepared in this fashion are unaffected by solvents, salts, chaotropes or temperature [19]. We hypothesize that these stable nano-capsules act as cationic nucleation centers for the DNA, which coat the surface perhaps through winding, analogously to how histones compact DNA to form nucleosomes [25, 26]. The cationic lysine residues exposed on the outer surface of BAPCs bind electrostatically to the repeating negatively charged phosphate groups present in DNA. Transmission electron microscopy (TEM) images revealed a complete, uniform coating of a single BAPCs surface with what appears to be a double strand DNA (Fig. 1A) or in clusters (Fig. 1B), confirming that a multi-molecular process should exist where more than one BAPC and most likely one DNA plasmid molecule are involved in the supra-molecular structure of the nanoparticles.

A dried supercoiled 4.7 kb plasmid DNA visualized with atomic force microscope (AFM) showed an estimated size of ~400 nm [20]. However, free soluble DNA molecules generally adopt much larger sizes [27,28]. For a single 20–30 nm BAPC, the curvature may be too high for a DNA chain to wrap tightly however, since the bending energy is inversely proportional to the square of the bending circle radius [27], bending of DNA around larger nanoparticle clusters requires much lower energies.

This might explain the presence predominantly of clusters with average size between 100 and 250 nm. The presence of both single and clustered BAPCs-DNA nanoparticles indicates that the DNA can assume several modes of associating with the BAPCs or that the assembly process may not have gone to completion. The single BAPC-DNA nanoparticles may be intermediates rather than endpoints (Fig. 1C).

AFM was also used to confirm the topologies of the BAPCs-DNA nanoparticles (Fig. 2A–B and Fig. 3S). We observed clusters with average size between 100 and 250 nm and single BAPCs-DNA complexes with particle size distribution between 50 and 80 nm - values in agreement with those obtained using TEM.

Based on the two different imaging techniques, BAPCs mixed with DNA form compact clusters with sizes ranging on average from 50 to 250 nm. Among several parameters such as particle shape, rigidity, surface properties and degradability, particle size is known to play an important role for intracellular uptake and subsequent transfection efficiency. Rejman et al. [29], demonstrated that nanoparticles with a size of 50 nm are taken up 34 times faster than 100 nm particles and 810 times faster than 500 nm particles. Thus, BAPC-DNA nanoparticles appear to fit into a suitable size range compatible with the in vitro cellular uptake.

To further evaluate the biophysical properties of the BAPCs-DNA nanoparticles, we measured the particle size and zeta potential of several formulations by dynamic light scattering (DLS). We analyzed the BAPCs-DNA complexes at different (N:P) charge ratios. The N:P charge ratio for a given complex is defined as the number of protonated amino groups (NH₃⁺) contained in the tetra-lysine portion of the branched peptides (even though not all are present on the outer surface of the BAPCs) and the number of charged phosphates (PO₄⁻) present in the plasmids used. Formulations with N:P ratios of 2.6, 10.4, 20.8 and 26 displayed an average size of ~150 nm and ~250 nm for the N:P = 1.3 (Fig. 3A). These results are in accordance to the particle size observed in TEM (Fig. 1) and AFM (Fig. 2 and Fig. 3S). The zeta potential (ZP) of the nanoparticles increased at higher peptide concentrations

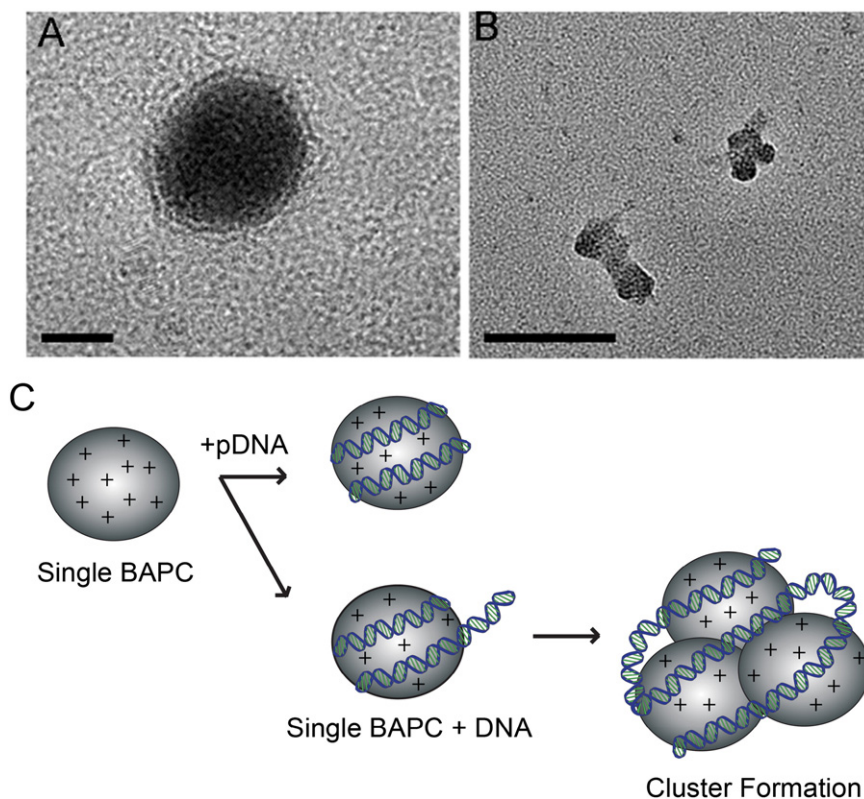


Fig. 1. TEM images of the BACP:DNA nanoparticles at N:P = 20.8. (A) Single BAPCs interacting with pDNA. Scale bar = 10 nm. (B) Cluster of BAPCs interacting with DNA. Scale bar = 100 nm. (C) Schematic representation of potential BAPC-DNA interactions.

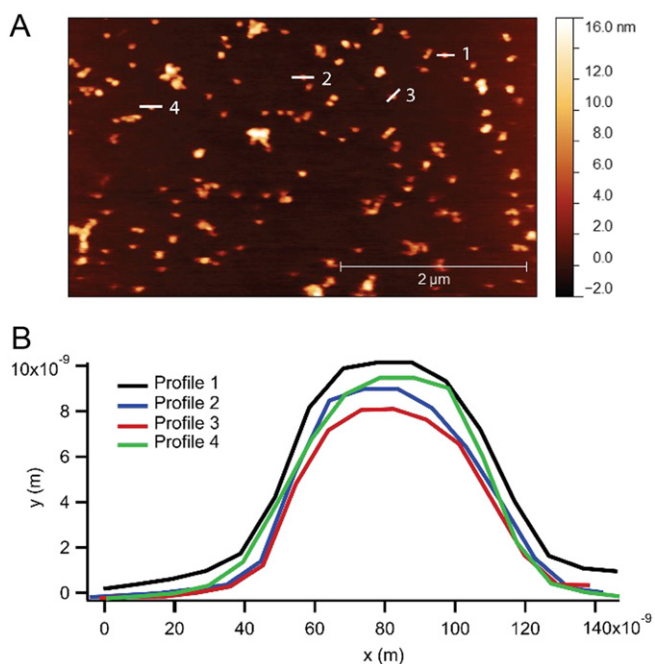


Fig. 2. AFM image analysis of the BACP-DNA nanoparticles at N:P = 20.8. (A) $5 \times 3 \mu\text{m}$ image of the nano-structures formed. (B) Cross sectional analyses of the numbered nano-structure shown in panel A.

demonstrating the efficient neutralization of the DNA in all the tested formulations (Fig. 3B). Neutral and positive ZP's improve cellular uptake. HeLa cells in suspension have been reported to have very low resting potentials (from -15 to -44 mV) [30] and supports the notion that the negative charge of the DNA needs to be sufficiently neutralized for efficient uptake [31].

3.2. In vitro transfection efficiency of BAPCs coupled with dsDNA

The ability of nano-sized BAPCs to deliver plasmid DNA in vitro was assessed by incubating cells with peptide-DNA nanoparticles at different N:P ratios. HeLa cells were incubated with BAPCs coated with a 4.7 kb GFP-encoding plasmid for 4 h in Opti-MEM® I Reduced Serum Media at N:P ratios ranging from 1.3 to 41.6. The ratios that showed the highest transfection efficiencies were 10.4, 20.8 and 41.6 yielding values of $(30.29\% \pm 1.59, 50.12\% \pm 2.5, \text{ and } 47.55\% \pm 1.65)$ respectively (Fig. 4A). To determine the influence of the incubation time on N:P

ratios 10.4 and 20.8, HeLa cells were also incubated with the BAPCs-DNA complexes for periods ranging from 2 h to 12 h. Optimal rates were obtained with incubation times of 4 and 6 h (Fig. 4S A). Different buffers were also evaluated in the absence and presence of CaCl_2 (1 mM). Addition of CaCl_2 (1 mM) promoted a small, but not statistically significant, increase in the number of transfected cells over those incubated with the nanoparticles in the absence of the salt (Fig. 4S B). Maximal transfection rates ($\sim 55\%$) for HeLa cells were achieved using DNA-complexed to BACP nanoparticles at a N:P ratio of 20.8 and an incubation time of 4 h with cells kept in Opti-MEM® I Reduced Serum Media containing 1 mM of CaCl_2 (Fig. 4A–B). We subsequently tested the ability of BAPCs to deliver larger plasmids; pCMV-SD95-21-GFP (19.4 kb) into a different cell line (HEK-293). For this cell line the highest transfection rates ($\sim 25\%$) were achieved using a N:P ratio of 26 with an incubation time of 4 h with cells kept in Opti-MEM® I (Fig. 4C–D). The plasmid pCMV-SD95-21-GFP encodes the entire genome for the North American type I porcine and reproductive syndrome virus (PRRSV). As observed in earlier publications [32], delivery and expression of this plasmid resulted in the shedding of competent RNA virus. This result indicates that BAPCs could find application in delivering vaccines derived from cDNA of attenuated virus thus eliminating the need for large production of protein inoculants. As a positive control, cells were transfected with the commercial reagent Lipofectin® using conditions optimized for each cell line. Quantification of the transfection efficiencies were monitored using fluorescence activated cell sorting (FACS). Propidium iodide (PI) was used to identify and then exclude dead cells from the analysis. Additionally, the in vitro cytotoxicity of the BAPCs-DNA nanoparticles was also evaluated in HeLa cells based on cell death entry of trypan blue (Fig. 5S A). The results showed that cell viability is minimally affected at the N:P ratio that produced the highest transfection efficiency while for the lipid-based transfection reagent, up to 40% of the cells did not survive the treatment. Confocal microscopy showed normal morphologies for those cells that were treated with BAPCs-DNA nanoparticles whereas those treated with Lipofectin® displayed abnormal cell structures (5S B–E).

3.3. In vivo delivery of a DNA vaccine encoding an HPV-16 oncoprotein

After evaluating the transfection efficiency and toxicity of the DNA-coated BAPCs in vitro, we tested the nano-sized complexes ability to deliver DNA in vivo. For that purpose, we tested a DNA vaccine that encodes the HPV-16 E7 oncoprotein (pgDE7) [22]. This vaccine has shown control in the proliferation of tumor cells expressing HPV-16 oncoproteins (TC-1 cells) grafted in C57BL/6 mice [22]. The pgDE7 plasmid was incubated with conformationally constrained BAPCs at N:P

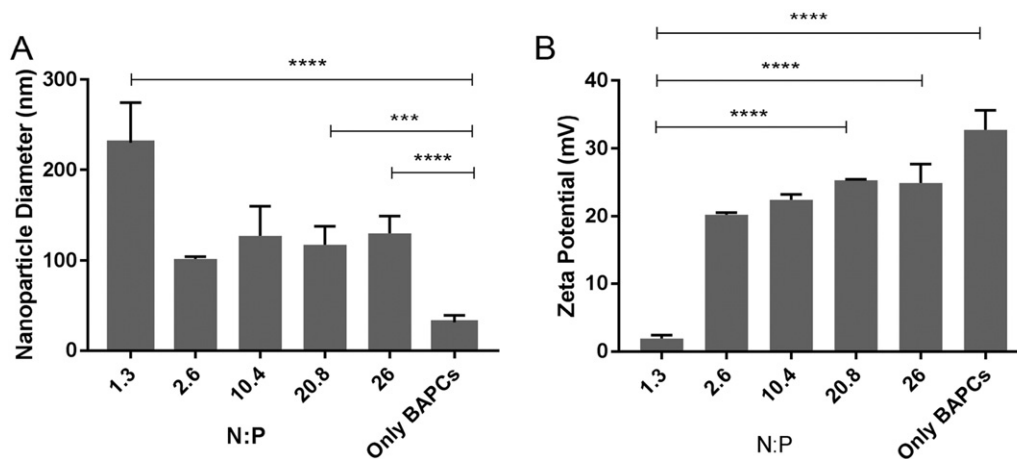


Fig. 3. Dynamic light scattering (DLS) and zeta potential data for different BAPCs-DNA formulations. (A) Size (z-average) and (B) zeta potential. Data represent mean values + SD of three experiments combined. Differences between values were compared by ANOVA using Bonferroni as post-test. Statistical significance: (***) $p < 0.001$; (****) $p < 0.0001$. Non-statistical significance (ns) was considered when $p > 0.05$.

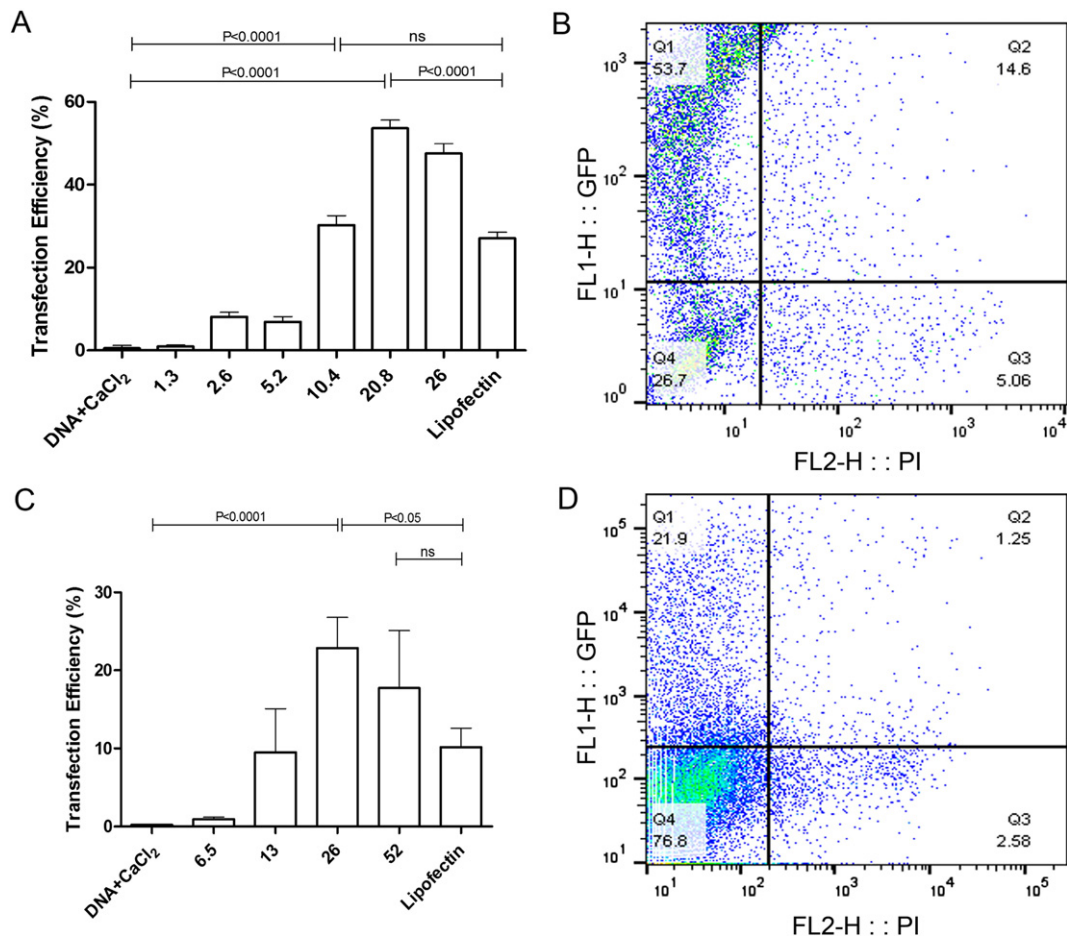


Fig. 4. In vitro transfection efficiency of BAPCs-DNA nanoparticles. (A) HeLa cells transfected with nanoparticles prepared at different peptide:DNA charge ratios (N:P) an incubation time of 4 h in reduced serum media and 1 mM CaCl₂. (B) Flow cytometry analysis of GFP-expressing HeLa cells after 48 h post transfection with BAPCs nanoparticles at N:P ratio 20.8 (C) HEK-293 cells transfected with nanoparticles prepared at different peptide:DNA charge ratios (N:P) an incubation time of 4 h in reduced serum media and 1 mM CaCl₂. (D) Flow cytometry analysis of GFP-expressing HEK-293 cells after 48 h post transfection with BAPCs nanoparticles at N:P ratio of 26. Data represent mean values + SD of four experiments combined. Differences between values were compared by ANOVA using Bonferroni as post-test. Non-statistical significance (ns) was considered when $p > 0.05$.

ratios of 10.4, 2.6 and 1.3. The complexed BAPCs-DNA was inoculated i.m. in mice, 3 days after inoculation of the TC-1 tumor cells. The negative control group was represented by sham treated mice. Other control groups received only naked pgDE7 plasmid and BAPCs complexed with a plasmid that does not encode pgDE7, to ensure that the anti-tumor protection is induced by the pgDE7 (Fig. 5A). Mice immunized with BAPCs coated with pgDE7 at N:P ratios higher than 2.6 did not efficiently control tumor growth. Animals inoculated with 2.6 ratio showed similar protection level compared with the group treated with naked pgDE7. BAPCs-DNA nanoparticles at N:P ratio of 10.4, which demonstrated enhanced transfection efficiency compared to DNA alone, displayed tumors that reached the size of ~1.0 cm, almost 30 days after transplantation of TC-1 cells, showing no statistical difference when compared with the non-vaccinated (control) mice and the 1.3 pGFP group. In contrast, mice immunized with pgDE7-coated BAPCs at N:P of 1.3 managed to constrain tumor growth up to one month after transplantation of the TC-1 cells. In addition, the survival time was enhanced by two-fold in comparison to that observed in the non-complexed DNA group (Fig. 5B). Immunization with BAPCs coated with pgDE7 at 1.3 N:P ratio also enhanced the number of E7-specific cytotoxic lymphocytes with regard to mice immunized with the same amount of DNA vaccine without BAPCs (Fig. 5C). It is noteworthy that only the 1.3 N:P ratio showed the least positive zeta potential value (2 mV) compared to the other preparations (Fig. 3B). These results might be associated with very low cytotoxicity and little or no tendency for aggregation promoting higher gene expression of the pDNA in vivo, as observed with other

nanoparticles presenting neutral zeta potential [33,34]. The particle size range obtained by DLS (~250 nm) for this formulation is comparable to previous reports on particulate DNA vaccine delivery systems [35].

3.4. Mouse DC activation by BAPCs-DNA nanoparticles

We have also analyzed the capacity of BAPCs-pgDE7 complexes to activate antigen presenting cells (APCs), a key step in the activation of T cell responses which are directly responsible for controlling tumor growth in the TC-1 tumor model [22]. Particulate carriers are known to enhance the immunogenicity of DNA vaccines by facilitating uptake by APCs, such as dendritic cells (DCs) [36,37,38]. Indeed, particles up to 500 nm are efficiently engulfed by DCs and result in activation of cytotoxic lymphocytes capable of recognizing and lysing tumor cells [39, 40]. DCs isolated from spleen of naïve C57BL/6 mice were incubated with the pgDE7-BAPCs and the expression of surface co-stimulatory receptor molecules (CD40, CD80 and CD86) was measured. Under our experimental conditions, DCs incubated with BAPCs-pgDE7 complexes showed augmented expression of co-stimulatory molecules, reaching similar levels as those observed after incubation with bacterial lipopolysaccharide (LPS), a potent activator of DCs (Fig. 6A–C). In contrast, no activation of co-stimulatory molecules was detected on DCs exposed to naked plasmid DNA or BAPCs not associated with DNA (Fig. 6A–C), which ruled out the possible effects associated with LPS contamination in DNA and BAPCs preparations. Moreover, DCs stimulated with the pgDE7-BAPCs secreted enhanced amounts of the pro-inflammatory

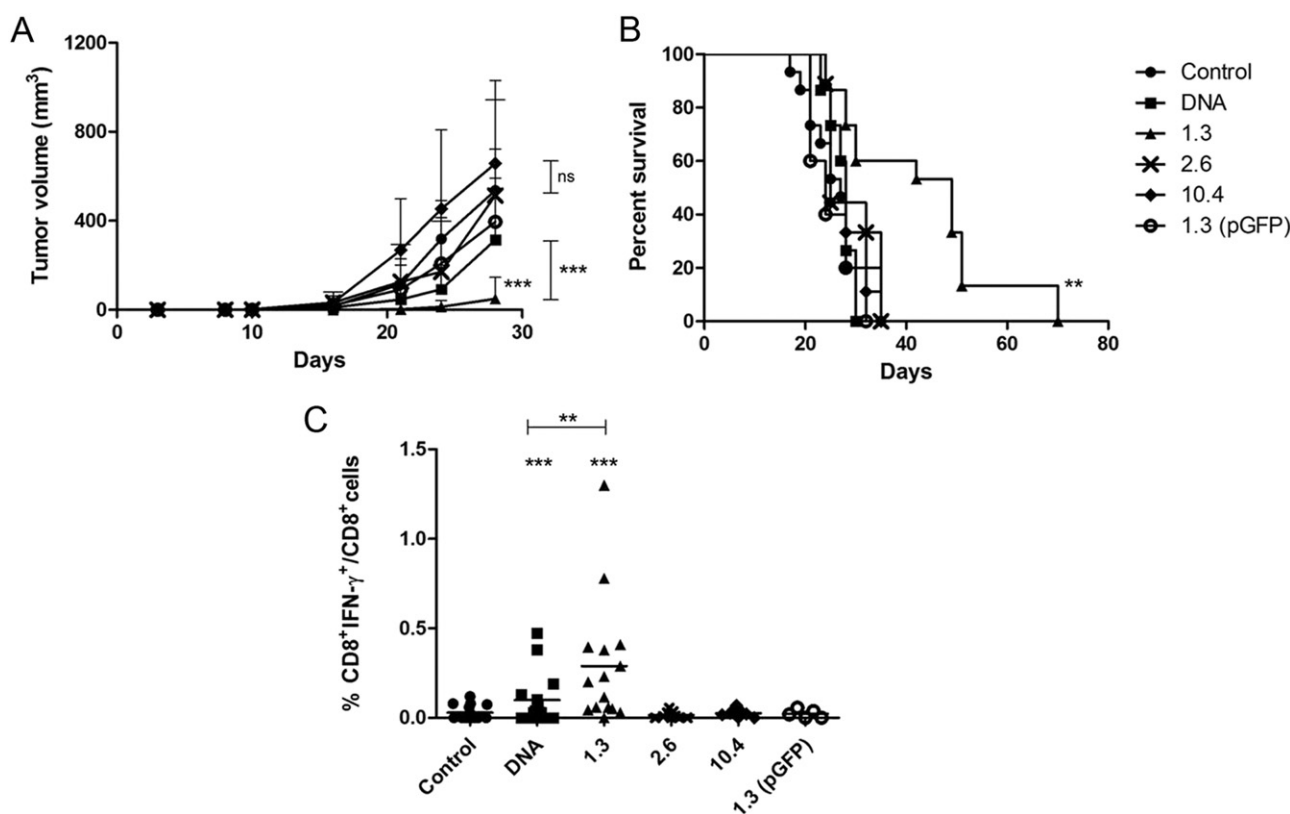


Fig. 5. Antitumor effect and survival curves of mice immunized with BAPCs-DNA nanoparticles at different N:P ratios. C57BL/6 mice were immunized i.m. with plasmid DNA (40 μ g) 3 days after injection of tumor cells (TC-1) complexed with or without BAPCs at 1.3, 2.6 and 10.4 charge ratios (N:P). The sham-treated group was inoculated with PBS based on the same inoculation regimen. The 1.3 (pGFP) group received 40 μ g of pGFP plasmid, used as a negative control for the vaccine. (A) Mean values of tumor size (mm³) progression + SD values until day 30. (B) Survival rates within 70 days after the TC-1 injection. Data is based on four independent experiments. (C) Intracellular IFN- γ staining of CD8⁺ T lymphocytes after *in vitro* stimulation with E7-derived MHC-I-specific RAHYNIVTF peptide (amino acids 49–57) of peripheral blood mononuclear cells (PBMCs) monitored by flow cytometry and expressed as percentage of CD8⁺IFN- γ ⁺ cells of total CD8⁺ T cell. The mean values that were used to compile these graphs can be found in supplementary material, Tables 1–3.

cytokines TNF- α and IL-6 that promote APC maturation and activation of cells involved in the adaptive immune response. In contrast, the production of IL-10, a suppressive cytokine associated with the activation of tolerogenic APCs, while moderately enhanced in the supernatants of DCs stimulated with BAPCs-DNA nanoparticles, was approximately 10-fold lower than those observed for TNF- α and IL-6, which is indicative of a cytokine balance shifted towards a pro-inflammatory environment (Fig. 6D). DCs stimulated with the same amount of pgDE7 or BAPCs alone were not affected as evaluated by the secretion of any of these cytokines. Our results indicate that coupling a plasmid DNA vaccine with BAPCs promote activation of DCs and, therefore, better prepared these cells for the subsequent activation of cytotoxic T lymphocytes (CTL) [41,42]. CTL, particularly CD8⁺ T cells, are key components of the immune system in controlling tumors [43,44]. Importantly, the secretion of TNF- α and IL-6, in combination with reduced secretion of immune suppressive cytokines (IL-10) by APCs may affect activation of CD8⁺ T lymphocytes as well as macrophages and natural killer cells, that also play relevant roles on the control of tumor cells growth.

3.5. *In vivo* toxicity assay of BAPCs-DNA nanoparticles

To test the *in vivo* toxicity of BAPCs coated with DNA at different N:P ratios, mice were inoculated i.m. with one dose of pgDE7-coated BAPCs. Blood samples collected from immunized mice were tested for the presence of aspartate (AST) and alanine (ALT) transaminases, and lactate dehydrogenase (LDH) (Fig. 7), which are recognized as markers of liver or general tissue damages. Only mice treated with free BAPCs and BAPCs associated with pGFP showed increased AST serum levels with regard the control group. None of the other tested groups

displayed abnormal values for these markers when compare with the control group up to 7 days after administration. DNA delivery systems based on nanoparticles, including gold-based nanomaterials and DNA-liposome complexes, often induce *in vivo* toxic effects, which vary accordingly to the dimensions and surface chemistry of the particles [45, 46]. Nonetheless, our results demonstrate that the DNA-coated BAPCs at N:P = 1.3 do not show detectable systemic toxicity and, thus, may be compatible with *in vivo* applications.

4. Discussion

Here we report the ability of nano-sized DNA-BAPCs to safely deliver plasmid DNA both *in vitro* and *in vivo*. *In vitro*, DNA-BAPCs nanoparticles transfected cells in culture with higher efficiency than that observed with a popular lipid-based commercial product and with less cytotoxicity. *In vivo*, they induce immune modulatory effects leading to enhancement of the anti-tumor effects of a DNA vaccine in a murine model. The non-complexed peptide nanoparticles, (~20–30 nm in diameter), were pre-formed in water at room temperature and subsequently incubated at 4 $^{\circ}$ C and then returned to RT. This protocol yields the conformationally constrained nanoparticles that are completely resistant to disassembly in organic solvents [19]. BAPCs prepared using other temperature regimes did not perform well in delivering dsDNA *in vivo*. Comparable to how histones compact DNA to form nucleosomes [23], the conformationally constrained BAPCs interact with plasmid DNA acting as a cationic nucleation centers with the negatively charged DNA coating the outer surface, generating peptide-DNA nanoparticles with sizes ranging between 50 and 250 nm. HeLa cells transfected *in vitro* with the BAPCs-DNA complexes showed transfection frequencies

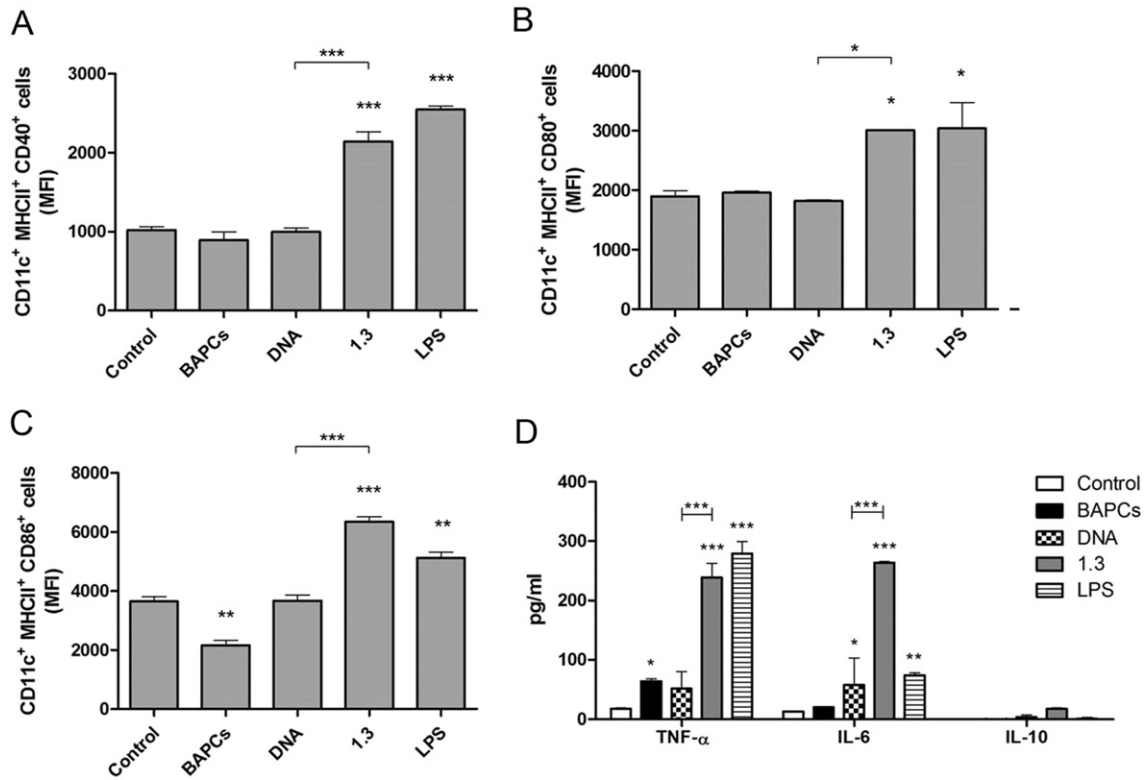


Fig. 6. In vitro activation of dendritic cells after incubation with BAPCs-DNA nanoparticles. DCs (3×10^5 cells) from naïve mice lymphoid organs were incubated for two days with PBS (control), only BAPCs at 100 μ M, DNA (10 μ g of pgDE7), BAPCs-DNA nanoparticles at N:P charge ratio of 1.3 and LPS (100 ng/mL). The surface expression levels of activation markers were measured by flow cytometry after gating in CD11c⁺ (PE) MHCII⁺ (FITC) cells shown as Median Fluorescence Intensity (MFI) bar graphs of CD40, CD80 and CD86 (APC) markers (A, B and C). (D) TNF- α , IL-6 and IL-10 cytokine induction (pg/mL) in cell culture supernatants. Data represent mean values +SD of two experiments combined. Statistical significance: (*) $p < 0.05$, (**) $p < 0.01$, (***) $p < 0.001$ versus Control group or as indicated in the bars (ANOVA, Bonferroni post-test).

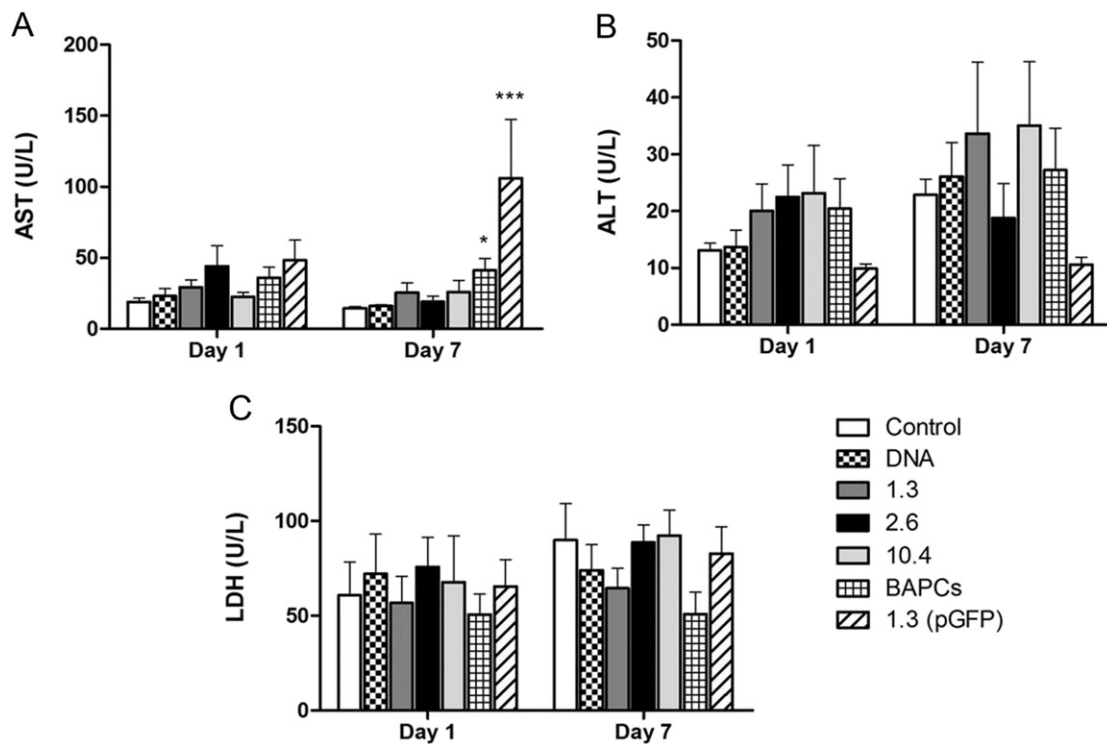


Fig. 7. Toxicity analysis of mice immunized with BAPCs-pgDE7 nanoparticles. C57BL/6 mice were immunized i.m. with naked DNA (40 μ g of pgDE7), BAPCs-pgDE7 nanoparticles at N:P ratio of 1.3, 2.6 and 10.4. Additionally, we tested a group treated with only BAPCs (without the pgDE7 plasmid) at 800 μ M and BAPCs-pGFP nanoparticles at N:P ratio of 1.3. The sham-treated group (control) received PBS at the same conditions. Individual sera were collected at day 1 or 7 after the immunization and analyzed for AST and ALT transaminases or LDH. Data represent mean values + SD of three experiments combined. Statistical significance: (*) $p < 0.05$, (***) $p < 0.001$ versus Control group (ANOVA, Bonferroni post-test).

approaching 55% (higher than cells treated with Lipofectin®). Notably, the size of the DNA constructs that can be delivered successfully can be larger since dsDNA can form complexes with the exterior surface of one or more BAPC particles. For this study, we delivered a 19.4 kb plasmid achieving significantly higher transfection efficiencies than those reached with cationic lipids. We tested the *in vivo* transfection performance of BAPCs with a plasmid DNA encoding an oncoprotein of HPV-16, previously used as a therapeutic anti-tumor vaccine. Administration of DNA-BAPC nanoparticles to mice showed that high N:P ratios, compatible with optimal HeLa and HEK-293 cell transfection effects, did not improve the protective immunity of the DNA vaccine. However, a lower N:P ratio resulted in substantial *in vivo* anti-tumor effects.

This results demonstrated that the N:P ratio has to be adjusted for each cell type and application purpose. It is noteworthy that the 1.3 N:P ratio showed the least positive zeta potential (~2 mV) compared to the other preparations. Bragonzi et al. [47] showed that large or highly positively charged nanoparticles are trapped in the lung and do not enter systemic circulation. Additionally, neutral zeta potentials are associated with low cytotoxicity, reduced plasma protein adsorption and little or no tendency for aggregation [33,34,48,49]. This may explain why the N:P = 1.3 ratio was the formulation that efficiently controlled tumor growth *in vivo*. The size, shape and degradability of nanoparticles, could all influence for *in vivo* gene delivery. Other parameters such as coronal effects and the resting potential of cells can also impact the nanoparticle performance. By testing additional constructs with multiple cell types in the near future we hope to determine additional underlying physical determinants.

We demonstrated that BAPC-DNA complexes activate DCs, which are responsible for activation and antigen presentation to effector cytotoxic T cells. Furthermore, the DNA-loaded BAPCs, at the most effective *in vivo* concentration, showed no detectable toxic effects, as evaluated by some critical tissue injury biomarkers. Moreover, as showed in the present study, the administration of BAPCs complexed with a DNA vaccine (pgDE7), conferred protection to tumors cells expressing HPV-16 oncoproteins. BAPC complexation with pgDE7 resulted in the increase in the numbers of antigen-specific CD8⁺ T cells and delayed tumor growth in mice previously grafted with TC-1 tumor cells. Together, these results indicate that the complexation of plasmid DNA to nano-sized BAPCs represents a promising non-viral gene delivery approach for *in vitro* transfection of mammalian cells and for the *in vivo* activation of immune responses.

Acknowledgments

General: We acknowledge ACR Moreno and BFMM Porchia for their contribution on the DC activation assays. We also appreciate the technical assistance of CBS Ferreira and CA Silva from the Microbiology Department and the Department of General Physics of University of Sao Paulo, Brazil.

Funding: This is publication **15-403-J** from the Kansas Agricultural Experiment Station. Partial support for this project was provided by the Terry Johnson Cancer Center at Kansas State University, The Center of Excellence for Emerging and Zoonotic Animal Diseases (CEEZAD) at Kansas State University and the Fundação de Amparo à Pesquisa do Estado de São Paulo - FAPESP (2013/15360-2).

Competing interests: The authors declare that they have no competing interests.

Data and materials availability: All data needed to evaluate the conclusions in the paper are present in the paper and/or the Supplementary Materials.

Appendix A. Supplementary data

Supplementary data to this article can be found online at <http://dx.doi.org/10.1016/j.jconrel.2016.08.042>.

References

- [1] M.A. Kutzler, D.B. Weiner, DNA vaccines: ready for prime time? *Nat. Rev. Genet.* 9 (2008) 776–788.
- [2] H. Yin, R.L. Kanasty, A.A. Eltoukhy, A.J. Vegas, J.R. Dorkin, D.G. Anderson, Non-viral vectors for gene-based therapy, *Nat. Rev. Genet.* 15 (2014) 541–555.
- [3] A. Bolhassani, S. Safaiyan, S. Rafati, Improvement of different vaccine delivery systems for cancer therapy, *Mol. Cancer* 10 (2011) 1–20.
- [4] D.V. Schaffer, J.T. Koerber, K. Lim, Molecular engineering of viral gene delivery vehicles, *Annu. Rev. Biomed. Eng.* 10 (2008) 169–194.
- [5] M.A. Kotterman, D.V. Schaffer, Engineering adeno-associated viruses for clinical gene therapy, *Nat. Rev. Genet.* 15 (2014) 445–451.
- [6] B.D. Lichty, C.J. Breitbach, D.F. Stojdl, J.C. Bell, Going viral with cancer immunotherapy, *Nat. Rev. Cancer* 15 (2014) 445–451.
- [7] L.A. Avila, S.Y. Lee, J.M. Tomich, Synthetic *in vitro* delivery systems for plasmids DNA in eukaryotes, *J. Nanopharm. Drug Deliv.* 2 (2014) 17–35.
- [8] Y. Wang, P. Han, H. Xu, Z. Wang, A.V. Kabanov, Photocontrolled self-assembly and disassembly of block ionomer complex vesicles: a facile approach toward supramolecular polymer nanocontainers, *Langmuir* 26 (2010) 709–715.
- [9] A.V. Korobko, C. Backendorf, J.R. van der Maarel, Plasmid DNA encapsulation within cationic diblock copolymer vesicles for gene delivery, *J. Phys. Chem. B* 110 (2006) 14550–14556.
- [10] X. Gao, L. Huang, Potentiation of cationic liposome-mediated gene delivery by polycations, *Biochemistry* 35 (1996) 1027–1036.
- [11] M.D. Brown, A. Schatzlein, A. Brownlie, V. Jack, W. Wang, L. Tetley, A.I. Gray, I.F. Uchegbu, Preliminary characterization of novel amino acid based polymeric vesicles as gene and drug delivery agents, *Bioconjug. Chem.* 11 (2000) 880–891.
- [12] W.-J. Jeong, Y.-B. Lim, Macrocyclic peptides self-assemble into robust vesicles with molecular recognition capabilities, *Bioconjug. Chem.* 25 (2014) 1996–2003.
- [13] E.G. Bellomo, M.D. Wyrsta, L. Pakstis, D.J. Pochan, T.J. Deming, Stimuli-responsive polypeptide vesicles by conformation-specific assembly, *Nat. Mater.* 3 (2004) 244–248.
- [14] M.E. Martin, K.G. Rice, Peptide-guided gene delivery, *AAPS J.* 9 (2010) 18–29.
- [15] S. Gudlur, P. Sukthankar, J. Gao, L.A. Avila, Y. Hiromasa, J. Chen, T. Iwamoto, J.M. Tomich, Peptide nanovesicles formed by the self-assembly of branched amphiphilic peptides, *PLoS One* 7 (2012), e45374.
- [16] S.M. Barros, S.K. Whitaker, P.R. Sukthankar, S. Gudlur, M. Warner, E.I.C. Beltrão, J.M. Tomich, A review of solute encapsulating nanoparticles used as delivery systems with emphasis on branched amphiphilic peptide capsules, *Arch. Biochem. Biophys.* 596 (2016) 22–42.
- [17] P. Sukthankar, S. Gudlur, L.A. Avila, S.K. Whitaker, B.B. Katz, Y. Hiromasa, J. Gao, P. Thapa, D. Moore, T. Iwamoto, J. Chen, J.M. Tomich, Branched oligopeptides form nano-capsules with lipid vesicle characteristics, *Langmuir* 29 (2013) 14648–146454.
- [18] P. Sukthankar, L.A. Avila, S.K. Whitaker, T. Iwamoto, A. Morgenstern, C. Apostolidis, K. Liu, R.P. Hanzlik, E. Dadachova, J.M. Tomich, Branched amphiphilic peptide capsules: cellular uptake and retention of encapsulated solutes, *Biochim. Biophys. Acta* 1838 (2015) 2296–2305.
- [19] P. Sukthankar, S.K. Whitaker, M. Garcia, A. Herrera, M. Boatwright, O. Prakash, J.M. Tomich, Thermally induced conformational transitions in nascent branched amphiphilic peptide capsules, *Langmuir* 31 (2015) 2946–2955.
- [20] L.A. Avila, L.M.M. Aps, P. Sukthankar, N. Ploscaru, G. Gudlur, L. Šimo, R. Szoszkiewicz, Y. Park, S.Y. Lee, T. Iwamoto, L.C.S. Ferreira, J.M. Tomich, Branched amphiphilic cationic oligopeptides form peptiplexes with DNA: a study of their biophysical properties and transfection efficiency, *Mol. Pharm.* 12 (2015) 706–715.
- [21] Y. Zhang, A. Satterlee, L. Huang, *In vivo* gene delivery by nonviral vectors: overcoming hurdles? *Mol. Ther.* 20 (2012) 1298–1304.
- [22] M.O. Diniz, F.A. Cariri, L.M.M. Aps, L.C. Ferreira, Enhanced therapeutic effects conferred by an experimental DNA vaccine targeting human papillomavirus-induced tumors, *Hum. Gene Ther.* 24 (2013) 861–870.
- [23] Y. Li, L. Zhu, S.R. Lawson, Y. Fang, Targeted mutations in a highly conserved motif of the nsp1₁ protein impair the interferon antagonizing activity of porcine reproductive and respiratory syndrome virus, *J. Gen. Virol.* 94 (2013) 1972–1983.
- [24] D. Necas, P. Klapetek, Gwyddion: an open-source software for SPM data analysis, *Cent. Eur. J. Phys.* 10 (2012) 181–188.
- [25] R.P. Ghosh, R.A. Horowitz-Scherer, T. Nikitina, L.S. Shlyakhtenko, C.L. Woodcock, MeCP2 binds cooperatively to its substrate and competes with histone H1 for chromatin binding sites, *Mol. Cell. Biol.* 19 (2010) 4656–4670.
- [26] A.A. Zinchenko, K. Yoshikawa, D. Baigl, Damien, Compaction of single-chain DNA by histone-inspired nanoparticles, *Phys. Rev. Lett.* 95 (2005) 22–25.
- [27] J.P. Peters, L.J. Maher, DNA curvature and flexibility *in vitro* and *in vivo*, *Rev. Biophys.* 43 (2010) 23–63.
- [28] H.G. Garcia, P. Grayson, M. Inamdar, J. Kondev, P.C. Nelson, R. Phillips, J. Widom, P.A. Wiggins, Biological consequences of tightly bent DNA: The other life of a macromolecular celebrity, *Biopolymers* 85 (2007) 115–130.
- [29] J. Rejman, V. Oberle, I.S. Zuhorn, D. Hoekstra, Size-dependent internalization of particles via the pathways of clathrin- and caveolae-mediated endocytosis, *J. Biochem. J.* 377 (2004) 159–169.
- [30] X. Zhang, Y. Jin, M.R. Plummer, S. Pooyan, S. Gunaseelan, P.J. Sinko, Endocytosis and membrane potential are required for HeLa cell uptake of R1-CKTat9, a retro-inverso Tat cell penetrating peptide, *Mol. Pharm.* 3 (2009) 836–848.
- [31] S. Honary, F. Zahir, Effect of zeta potential on the properties of nano-drug delivery systems, *Trop. J. Pharm. Res.* 2 (2013) 265–273.
- [32] Y. Li, L. Zhu, S.R. Lawson, Y. Fang, Targeted mutations in a highly conserved motif of the nsp1₃ protein impair the interferon antagonizing activity of porcine reproductive and respiratory syndrome virus, *J. Gen. Virol.* 94 (2013) 1972–1983.

- [33] T. Merdan, K. Kunath, H. Petersen, U. Bakowsky, K.H. Voigt, J. Kopecek, T. Kissel, PEGylation of poly(ethylene imine) affects stability of complexes with plasmid DNA under in vivo conditions in a dose-dependent manner after intravenous injection into mice, *Bioconj. Chem.* 16 (2005) 785–792.
- [34] E. Blanco, H. Shen, M. Ferrari, Principles of nanoparticle design for overcoming biological barriers to drug delivery, *Nat. Biotechnol.* 33 (2015) 941–951.
- [35] V.B. Joshi, S.M. Geary, A.K. Salem, Biodegradable particles as vaccine delivery systems: size matters, *AAPS J.* 15 (2012) 85–94.
- [36] A. Monie, S.-W.D. Tsen, C.-F. Hung, T.-C. Wu, Therapeutic HPV DNA vaccines, *Expert Rev. Vaccines* 8 (2009) 1221–1235.
- [37] M.E.C. Lutsiak, D.R. Robinson, C. Coester, G.S. Kwon, J. Samuel, Analysis of poly(D,L-lactic-co-glycolic acid) nanosphere uptake by human dendritic cells and macrophages in vitro, *Pharm. Res.* 19 (2002) 1480–1487.
- [38] D.T. O'Hagan, N.M. Valiante, Recent advances in the discovery and delivery of vaccine adjuvants, *Nat. Rev. Drug Discov.* 2 (2003) 727–735.
- [39] J. Banachereau, R.M. Steinman, Dendritic cells and the control of immunity, *Nature* 392 (1998) 245–252.
- [40] M. Cella, C. Dohring, J. Samaridis, M. Dessing, M. Brockhaus, et al., A novel inhibitory receptor (ILT3) expressed on monocytes, macrophages, and dendritic cells involved in antigen processing, *Exp. Med.* 185 (1997) 1743–1751.
- [41] I. Mellman, G. Coukos, G. Drano, Cancer immunotherapy comes of age, *Nature* 480 (2011) 480–489.
- [42] A. Langenkamp, M. Messi, A. Lanzavecchia, F. Sallusto, Kinetics of dendritic cell activation: impact on priming of TH1, TH2 and nonpolarized T cells, *Nat. Immunol.* 4 (2000) 311–316.
- [43] T. Kawano, J. Cui, Y. Koezuka, I. Toura, Y. Kaneko, K. Motoki, H. Ueno, R. Nakagawa, H. Sato, E. Kondo, H. Koseki, M. Taniguchi, CD1d-restricted and TCR-mediated activation of valpha14 NKT cells by glycosylceramides, *Science* 278 (1997) 1626–1629.
- [44] M.J. Welters, G.G. Kenter, S.J. Piersma, A.P. Vloon, M.J. Löwik, D.M. Berends-van der Meer, J.W. Drijfhout, A.R. Valentijn, A.R. Wafelman, J. Oostendorp, G.J. Fleuren, R. Offringa, C.J. Melief, S.H. van der Burg, Induction of tumor-specific CD4⁺ and CD8⁺ T-cell immunity in cervical cancer patients by a human papillomavirus type 16 E6 and E7 long peptides vaccine, *Clin. Cancer Res.* 14 (2008) 178–187.
- [45] H. Lv, S. Zhang, B. Wang, S. Cui, J. Yan, Toxicity of cationic lipids and cationic polymers in gene delivery, *J. Control. Release* 114 (2006) 100–109.
- [46] S.A. Love, M.A. Maurer-Jones, J.W. Thompson, Y.S. Lin, C.L. Haynes, Assessing nanoparticle toxicity, *Annu. Rev. Anal. Chem.* 5 (2012) 181–205.
- [47] A. Bragonzi, G. Dina, A. Villa, G. Calori, A. Biffi, C. Bordignon, B.M. Assael, M. Conese, Biodistribution and transgene expression with nonviral cationic vector/DNA complexes in the lungs, *Gene Ther.* 7 (2000) 1753–1760.
- [48] E. Pridgen, L.K. Molnar, O.C. Farokhzad, Factors affecting the clearance and biodistribution of polymeric nanoparticles frank Alexis, *Mol. Phar.* 5 (2008) 505–515.
- [49] L. Hongtao, S. Zhang, B. Wang, S. Cui, J. Yan, Toxicity of cationic lipids and cationic polymers in gene delivery, *J. Control. Release* 114 (2006) 100–109.